Journal of Ethnopharmacology 161 (2015) 163–169

Contents lists available at ScienceDirect

Journal of Ethnopharmacology

journal homepage: www.elsevier.com/locate/jep

Research Paper

Effects of Xie-Zhuo-Chu-Bi-Fang on miR-34a and URAT1 and their relationship in hyperuricemic mice

Wei-Feng Sun [a,*,1], Ming-Min Zhu [b], Jing Li [a,b], Xian-Xian Zhang [a], Ying-Wan Liu [a], Xin-Rong Wu [a,**,1], Zhi-Gang Liu [a]

[a] Department of Traditional Chinese Medicine, General Hospital of Guangzhou Military Command of PLA, Guangzhou 510010, China
[b] Guangzhou University of Chinese Medicine, Guangzhou 510006, China

ARTICLE INFO

Article history:
Received 13 October 2013
Received in revised form
14 November 2014
Accepted 1 December 2014
Available online 19 December 2014

Chemical compounds studied in this article:
Astilbin (Pubchem CID: 119258)
Colchicine (Pubchem CID: 6167)
Ecdysterone (Pubchem CID: 5459840)

Keywords:
Hyperuricemia
Kidney
miR-34a
URAT1

ABSTRACT

Ethnopharmacological relevance: Xie-Zhuo-Chu-Bi-Fang (XZCBF) is an empirical formula that was developed based on the principles of traditional Chinese medicine, for the therapeutic purpose of treating hyperuricemia. XZCBF has been clinically utilized in the Department of Traditional Chinese Medicine at General Hospital of Guangzhou Military Command of PLA for many years and has exhibited favorable efficacy. The aim of the study is to evaluate the effects of XZCBF on the expression of uric acid transporter 1 (URAT1) and miR-34a in hyperuricemic mice and to determine, the correlation between the two expression levels.

Materials and methods: A hyperuricemic animal model was created by administering adenine and allantoxanic acid potassium salt to mice. The blood uric acid levels were measured in these model mice after treatment with XZCBF for 15 days. The potential targets of miR-34a were screened. The expression levels of miR-34a and URAT1 in the renal tissues collected from the model mice were determined by quantitative real-time polymerase chain reaction (qRT-PCR) analysis, and their correlation was further established by immunohistochemistry and in situ hybridization.

Results: The uric acid levels in the model mice were significantly higher than those in the blank controls ($P < 0.05$). These levels were significantly lower in the three groups receiving different doses of XZCBF ($P < 0.05$), which was, in agreement with the downregulation of URAT1 and the upregulation of miR-34a in each group. The mRNA expression level of URAT1 was positively correlated with the concentration of uric acid but, negatively correlated with the expression level of miR-34a.

Conclusions: The ability of XZCBF to facilitate the excretion of uric acid and to lower its level in the model group was mediated by the upregulation of miR-34a and the inhibition of URAT1 mRNA expression, which suggests that XZCBF could be an option for the treatment of hyperuricemia in mice.

1. Introduction

Epidemiological surveys from various countries have shown that the prevalence of hyperuricemia and gout has risen significantly, while the age of incidence has decreased (Roddy et al., 2007; Wu et al., 2008). The asymptomatic period of hyperuricemia is relatively long; however, deposits of uric acid salt cause injury to tissues and internal organs, which have been closely associated with conditions such as renal insufficiency, cardiovascular disease and hyperlipidemia.

Hyperuricemia is characterized by a state of over-saturation of extracellular urate, which is caused by a malfunction in purine metabolism or a decrease in uric acid production. Uric acid is a product of purine metabolism, and a large majority is excreted in the urine through four steps, described as ultrafiltration, reabsorption, secretion, and post-secretion reabsorption. Ninety-eight percent of glomerular-filtered uric acid is reabsorbed by the renal tubules, a process that depends on human urate acid transporter 1 (hURAT1, SLC22A12). hURAT1 is a transporter protein that has been shown to be closely related to the reabsorption of uric acid. This transporter is selectively localized on the luminal surface of the epithelial lining along the proximal renal tubules (Wang, 2004), where it maintains the electrical balance across the cell membrane by transporting uric acid in exchange for anions (Hong et al., 2005). Nonsynonymous mutations in the coding region of

* Correspondence to: Department of Traditional Chinese Medicine, General Hospital of Guangzhou Military Command of PLA, No.111 Liuhua Road, Yuexiu District, Guangzhou (510010), China. Tel.: +86 20 36653520.
** Corresponding author. Tel.: +86 20 88653476.
E-mail addresses: sunwf3@sina.com (W.-F. Sun), gzwxrong@yahoo.com (X.-R. Wu).
[1] Contributed equally to this work.

http://dx.doi.org/10.1016/j.jep.2014.12.001

SLC22A12 leading to loss of function were reportedly found in patients diagnosed with familial hypouricemia, and downregulation of URAT1 could result in elevated excretion of uric acid (Cheong et al., 2008).

The promoter of uric acid excretion, benzbromarone, is an effective inhibitor of URAT1, which facilitates the excretion of uric acid by directly inhibiting URAT1 on the top surface of the renal tubules. However, benzbromarone has adverse effects including functional impairment of the liver, gastrointestinal reactions, and rash. Traditional Chinese medicine (TCM) has definite curative effects in the treatment of hyperuricemia without serious adverse effects, and an understanding of the underlying mechanism of TCM has important practical significance.

Xie-Zhuo-Chu-Bi-Fang (XZCBF) is an empirical formula that was developed based on the principles of TCM and is used to treat hyperuricemia. This formula has obtained a national invention patent (Patent no.: ZL 2007 1 0032363.3). XZCBF consists of the following herbs: *Smilax glabra* Roxb., rhizome (tu fu ling, Smilacis Glabrae Rhizoma), *Heterosmilax japonica* Kunth, rhizome (bi xie, Heterosmilacis Rhizoma), *Cremastra appendiculata* (D.Don) Makino, rhizome (shan ci gu, Cremastrae Pseudobulbus), *Vaccaria hispanica* (Mill.) Rauschert, seed (wang bu liu xing, Vaccariae Semen), and *Achyranthes bidentata* Blume, root (niu xi, Achyranthis Bidentatae Radix). XZCBF has been applied clinically in the Department of TCM at General Hospital of Guangzhou Military Command for many years, and its overall efficacy rate was statistically estimated to reach approximately 90% (Sun et al., 2009). For more convenient use, we developed a granular form of XZCBF: Compound Tufuling Granules (approved by Guangdong Food and Drug Administration, license no. Guang Zhi Zi 2011-F01009).

According to the theory of Chinese Materia Medica (Chinese Pharmacopoeia Commission, 2010), *Smilax glabra* Roxb., *Heterosmilax japonica* Kunth, *Vaccaria hispanica* (Mill.) Rauschert and *Achyranthes bidentata* Blume can induce diuresis to dispel "Dampness" and "Turbidity"; *Smilax glabra* Roxb. and *Heterosmilax japonica* Kunth can smoothen joint movement to eliminate Impediment; *Cremastra appendiculata* (D.Don) Makino, *Vaccaria hispanica* (Mill.) Rauschert, and *Achyranthes bidentata* Blume can activate "Blood" and resolve "Stasis"; *Achyranthes bidentata* Blume can tonify the "Liver" and "Kidney", and conduct "Blood" downward. All of these effects are beneficial in the treatment of hyperuricemia and gout in TCM. To support the traditional use of XZCBF, many studies on the activities of these herbs have been performed. *Smilax glabra* Roxb. and its main active compound astilbin have anti-inflammatory, analgesic and diuretic effects (Zhang et al., 2004). *Heterosmilax japonica* Kunth can eliminate uric acid, and it has anti-inflammatory and analgesic effects (Fei et al., 2005, 2007). Colchicine, one of the active compounds in *Cremastra appendiculata* (D.Don) Makino (Shi et al., 2012), is an anti-inflammatory agent. In addition, it can reduce the risk of myocardial infarction in gout patients (Crittenden et al., 2012). *Vaccaria hispanica* (Mill.) Rauschert has vasodilatory effects (Jing et al., 2007). *Achyranthes bidentata* Blume has restorative effects on deficiencies of the immune system (Li and Li, 1997), has analgesic and anti-inflammatory effects, and invigorates the circulation (Gao et al., 2003).

Our previous study (Sun et al., 2011) demonstrated that XZCBF lowered uric acid levels in hyperuricemic mice that were administered adenine and allantoxanic acid potassium salt. The upstream microRNA regulatory mechanism was also examined. MicroRNAs are part of the long transcribed segments of RNA, and a mature microRNA binds to an RNA-mediated silencing complex that is similar to (or the same as) the complex that is involved in RNA interference, resulting in the downregulation of gene expression in vivo (Lewis et al., 2005; Wu et al., 2006). By screening microRNA spectrum, the expression levels of 32 genes were identified as being significantly different, and 3 genes (miR-34a, miR-122, and miR-146a) were closely associated with XZCBF. In addition, miR-34a was found to be capable of binding to the 3′UTR of URAT1, which is consistent with the inhibitory role of miR-34a that was identified in a sensor reporter assay. In this study, we located the binding site of miR-34a in URAT1 by predicting target sites and exploring the relationships between XZCBF, miR-34a, and URAT1 using biomedical approaches, including vector construction, immunohistochemistry, and in situ hybridization.

2. Materials and methods

2.1. Reagents

The following reagents were acquired: 97% allantoxanic acid potassium salt (Sigma-Aldrich, Shanghai), adenine (Sigma-Aldrich, Shanghai), a uric acid assay kit (liquid, enzymatic method; Eastern China Diagnostic [Shanghai] Co. Ltd), SYBR Green PCR Master Mix (TOYOBO Company, Japan), TRIzol® Reagent (Invitrogen, USA), anti-digoxigenin-AP (Roche, Switzerland), hsa-miR-34a (Exiqon, USA); anti URAT1 (rabbit IgG; Abbiotec, USA), secondary antibody (DAKO ChemMate™, Denmark), and a detection kit (DAKO Envision™, Denmark).

2.2. Chemicals

The herbs we used in this study were all commercially available as dry matter and were purchased from Nanhai Pengyang Pharmaceutical Co., Ltd. (Table 1). These herbs were identified by Professor Xin-Rong Wu (Pharmacy Department of General Hospital of Guangzhou Military Command, Guangzhou, China) and Director Hui-Chan Hou (Chinese Medicine Department of Guangzhou Institute for Drug Control, Guangzhou, China). Voucher specimens were deposited in the Herbarium of Guangzhou Institute for Drug Control. The dosages of the herbs in XZCBF are based on the theory of Chinese Materia Medica.

These herbs were processed into Compound Tufuling Granules by the Pharmacy Department of General Hospital of Guangzhou Military Command (10 g per bag, batch no.110916). The formulation was extracted and purified by water extraction and an alcohol sedimentation process (Liu et al., 2011a). The excipient of the granules was soluble starch (Xiangtan County Starch Products Co., Ltd., batch number: 20110116) and granule quality was assessed by thin layer chromatography (TLC) and high performance liquid chromatography (HPLC) (Liu et al., 2011b). Using HPLC, the content of ecdysterone (one main component of XZCBF) in the granules was determined to be 0.22 mg/g.

Benzbromarone was acquired from Longdengrui Pharmaceutical (Kunshan) Co. Ltd. (batch no. 110302).

Distilled water was added at the necessary concentrations for future use, and samples were shaken to ensure an equal distribution of the components prior to use.

Table 1
Information regarding the herbs.

Herbs	Origin (China)	Specimen no.	Dosage (g)
Smilax glabra Roxb., rhizome	Guangxi	01-2-2-4	35
Heterosmilax japonica Kunth, rhizome	Guangxi	15-1-2-1	18
Cremastra appendiculata (D.Don) Makino, rhizome	Guizhou	08-4-1-7	15
Vaccaria hispanica (Mill.) Rauschert, seed	Anhui	20-2-1-8	10
Achyranthes bidentata Blume, root	Henan	16-1-2-1	10

2.3. Equipment

A Hitachi-H7170 automatic biochemical analyzer (Hitachi, Japan), a quantitative PCR machine (ABI PRISM® 7500 Sequence Detection System, USA), a light microscope (Type: CX41, Olympus, Japan), a camera system (Type: MC30, Mingmeike Sci&Tech [Guangzhou] Co. Ltd., China), and a freezing microtome (Leica, Germany) were used.

2.4. miR-34a target -gene predictions and luciferase assay

The target genes of miR-34a were predicted by searching the TargetScan database online, and they were confirmed using the miRanda database.

To construct the vector for the luciferase assay, the concatemer of the miR-34a target sequence in the 3′UTR of URAT1 and its complimentary tandem sequence of "seeds" in miR-34a were cloned downstream of the luciferase gene, which was driven by the CMV promoter (Wu et al., 2006). The construct, together with a miR-34a mimic or non-relevant loop, was transfected into newly generated myocardiocytes. The cells were collected after 24 h, and their luciferase activity was measured using an Lmax multiwell luminometer.

2.5. Animal model and administration of chemicals

Sixty SPF Kunming male mice weighing 28 ± 2 g, provided by the Animal Center of General Hospital of Guangzhou Military Command, were fed normally. All of the study reports were guided by the Animal Center of General Hospital of Guangzhou Military Command, and the animal performance protocol was approved by the ethics committee of the institution.

Adenine was combined with allantoxanic acid potassium salt to create a model of hyperuricemia. The mice were randomized into 6 groups: XZCBF high-, medium- and low-dose groups; the benzbromarone group; the model group; and the blank control group. Adenine (0.1 g/kg) and 97% allantoxanic acid potassium salt (0.1 g/kg) were administered by gavage to each group (except for the blank control group) to create the hyperuricemic model; the blank control group was administered an equal volume of normal saline by gavage once per day, and the treatment period was 21 days.

The therapeutic drugs were administered on the 7th day of adenine and allantoxanic acid treatments. The corresponding drugs were administered to the XZCBF high-, medium- and low-dose groups, the benzbromarone group, and the model group. Compound Tufuling (*Rhizoma Smilacis* Glabrae) granules at doses of 6, 3, and 1.5 g/kg (equal to XZCBF doses of 37.5, 18.75, and 9.375 g/kg) were administered to the high-, medium- and low-dose groups, respectively. Because drug metabolism is not exactly the same between human and mice, we utilized 3 different doses of XZCBF to evaluate its efficacy. The concentrations of the extracts administered were calculated based on body surface area. Adult patients take Compound Tufuling Granules at a dose of 20 g per day, and the average weight of an adult is 60 kg. The body surface area conversion coefficient from humans to mice is 9.03; thus the normal dose (medium dose) of Compound Tufuling Granules administered to mice was $20/60 \times 9.03 \approx 3$ g/kg. The high dose is double the medium dose, and the low dose is half the medium dose. The benzbromarone group received 20 mg/kg benzbromarone, and an equal volume of normal saline was administered to the model and blank groups. Administration was performed once per day by gavage, and the treatment period was 15 days.

2.6. Blood uric acid analysis

Blood was drawn from the eyes of mice on the 22nd day of the experiment and was centrifuged in dry tubes at 3000 rpm for 10 min. The serum was separated, and the uric acid level was determined by the uricase method (Trinder's method).

2.7. qRT-PCR analysis of URAT1 and miR-34a expression in kidney tissue

Bilateral kidneys were harvested from the mice and pulverized in liquid nitrogen, and total RNA was obtained with a Trizol one-step RNA isolation kit. The expressions levels of URAT1 and miR-34a were analyzed following the protocols described below.

The RT reaction of URAT1 was performed in an RNase-free PCR tube using the following protocol: DEPC water was added to 1.0 μg of total RNA to achieve a volume of 12 μL; incubation at 85 °C for 5 min; addition of 0.5 μL of Oligo(dT)(Promega), 0.5 μL of random primer (Promega), 2.0 μL of 10 mM dNTP Mix, 0.5 μL of RNase inhibitor, 4.0 μL of 5 × M-MLV RT Buffer, and 0.5 μL of M-MLV; incubation of the 20 μL reaction solution at 30 °C for 10 min; incubation at 42 °C for 60 min; and incubation at 85 °C for 10 min.

qRT-PCR of miR-34a was performed using the stem-loop method. The reactions were performed in RNase-free PCR tubes as follows: DEPC water was added to 1.0 μg of total RNA to achieve a volume of 12 μL, incubation at 85 °C for 5 min. Another solution was made in a new RNase-free PCR tube with the following constituents: 2.0 μL of 10 mM dNTP (Promega), 0.5 μL of RNase inhibitor (Promega), 0.5 μL of miR-34a reverse transcription primers, 0.5 μL of U6 reverse transcription primers, 4.0 μL of 5 × buffer, and 0.5 μL of M-MLV (Promega). The solutions in the two PCR tubes were mixed and incubated at 42 °C for 60 min; then, the mixture was incubated at 85 °C for 10 min to inactivate the reverse transcriptase.

The sequences of the synthetic primers used in quantitative PCR are shown in Table 2. The reaction system consisted of the following components: 5.0 μL of cDNA (1:20), 0.5 μL of forward primer, 0.5 μL of reverse primer, 10 μL of 2 × SYBR Green PCR Master Mix, 4.0 μL of dH_2O.

The URAT1 and miR-34a amplification conditions were as follows: pre-denaturation at 95 °C for 5 min followed by 40 cycles of denaturation at 95 °C for 15 s, annealing at 60 °C for 15 s, and extension at 72 °C for 32 s, with a final extension at 72 °C for 5 min. The reaction was incubated at 4 °C for 10 min prior to plate reading. Melting curve analysis was performed at temperatures of 60–95 °C, with measurements performed at 0.4 °C. Each sample was assessed 3 times.

2.8. Immunohistochemistry and in situ hybridization of renal tissues

The expression of miR-34a was assessed using immunohistochemistry and in situ hybridization.

For immunohistochemistry, incubation was performed at 4 °C overnight, and secondary antibody incubation was performed at room temperature for 30 min, followed by developed with DAB, re-staining with hematoxylin, water washing, staining with blue dye, air

Table 2
Fluorescence quantitative PCR primer sequences.

Name	Primer Sequences (5′–3′)
URAT1-F1	5′ GAGGGAGACACGTTGACCAT
URAT1-R1	5′ TTGCTTCCTAGGGCTTGCA
18s rRNA-F	5′ CCTGGATACCGCAGCTAGGA
18s rRNA-R	5′ GCGGCGCAATACGAATGCCCC
mmu-miR-34a-F	5′ ACACTCCAGCTGGGTGGCAGTGTCTTAGCTGGT
miRNA-R[a]	5′ CTCAACTGGTGTCGTGGA
U6-F	5′ CTCGCTTCGGCAGCACA
U6-R	5′ AACGCTTCACGAATTTGCGT

[a] miRNA-R denoting microRNA downstream primers.

drying, and film sealing. The working concentration of the primary antibody was 1:2000.

For in situ hybridization, incubation was performed with proteinase K (40 μg/mL) at room temperature for 20 min, followed by incubation in the pretreatment buffer for 10 min, preliminary hybridization at 60 °C for 2 h, miRNA probe incubation at 90 °C for 5 min, hybridization at 60 °C overnight, sealing at room temperature for 1 h, incubation with anti-digoxin antibody at 4 °C overnight, and staining with BCIP/NBT in the dark for 4–48 h. The reaction was terminated with buffer at pH 8.0. Re-staining was performed with Nuclear Fast Red, and the film was sealed with neutral balsam. The final working concentration was 20 nM, and the hybridization temperature was 60 °C.

The digital images of URAT1 and miR-34a were analyzed using an IPP image analysis software. First, the gray unit was switched to the optical density unit in the program software, and the optical density analysis was performed with the yellow (stained URAT1) and purple (miR-34a -labeled) immunohistochemical stained regions as the areas of interest (AOIs). The density (mean) and integrated optical density (IOD) of the selected areas were measured.

2.9. Statistical analysis

The quantitative data are expressed as the mean ± standard deviation ($\bar{x} \pm SD$). The values were converted to square roots when the original standard error was large; multiple means were compared using one-way analysis of variance (ANOVA); the least-significant difference (LSD) method was applied when the variance was equal; and Dunnett's T3 test was performed when applied when the variance was not equal. Pearson's correlation method was used for the correlation analysis. All of the statistical analyses were performed with SPSS software 16.0 for Windows, with a significance level of $\alpha = 0.0500$.

3. Results

3.1. Targeted inhibition of URAT1 expression by miR-34a

The target genes of miR-34a were predicted using popular online microRNA target predicting tool: the TargetScan database. A miR-34a binding site located in the − 271–277 bp region of URAT1, 3′UTR was found, with the no.2–4 nucleotide "seeds sequence" precisely matching the target gene sequences, which indicated that miR-34a could inhibit the expression of URAT1. The result was checked and confirmed with those of another online tool, miRanda. We cloned mouse URAT1, 3′UTR into the multiple restrictive sites of the report vector psi-CHECK2 to construct recombinant vector psi-URAT1-miR34a-BS. We then cotransfected it, together with miR-34a mimics, into HEK293 (human embryonic kidney 293 cell line, a commonly used cell line in exogenous gene research) (Nadeau and Kamen, 2003). By assessing the expression level of the reporter gene, miR-34a was found to significantly inhibit the expression of luciferase in the psi-URAT1-miR34a-BS construct, strongly implying that miR-34a could inhibit the expression level of URAT1.

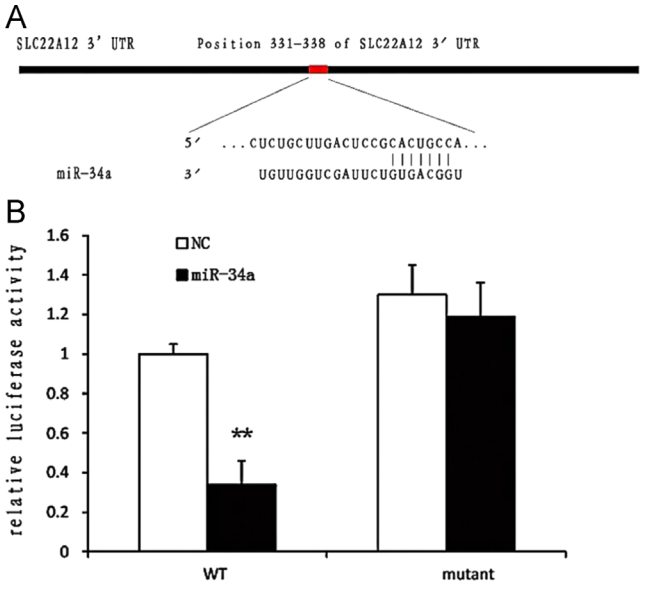

Fig. 1. Regulation of SLC22A12 by miR-34a. (A) A miR34a binding site was found in SLC22A12- 3′UTR using the microRNA target gene prediction tool TargetScan. (B) Negative control (NC) and miR-34a mimics, a firefly luciferase vector containing the wild type SLC22A12-3′UTR (WT), and a firefly luciferase vector containing the mutant SLC22A12-3′UTR were co-transfected into 293T cells, and the luciferase activity was assessed. $^{**}P < 0.01$.

3.2. MiR-34a targets SLC22A12

The predicted target site of miR-34a in SLC22A12-3′UTR was consistent with the effects of miR-34a on the luciferase activity of a luciferase- SLC22A12-3′UTR reporter construct in the 293T cell lines (a cell line derived from HEK293 cells that contains the T antigen, resulting in higher expression of transfected genes). Mutations in SLC22A12-3′UTR disrupted the potential miR-34a binding site, suppressing the inhibitory activity of miR-34a. Luciferase reporter constructs with mutations at the predicted miR-34a binding site within the SLC22A12-3′UTR, were generated. The wild-type SLC22A12-3′UTR construct and its mutant counterpart were transfected together with the negative control (NC) into 293T cells and the luciferase activity was examined 24 h after transfection ($^{**}P < 0.01$) (Fig. 1A and B).

3.3. Analysis of uric acid in urine

The blood uric acid level was 203.85 ± 43.34 μmol/L by the end of the study period, which was significantly different from that of the blank control (77.88 ± 24.92 μmol/L; $P < 0.05$). Oral administration of XZCBF lowered the concentration of uric acid to 110.63 ± 9.30, 125.34 ± 12.23, and 163.14 ± 29.56 μmol/L in the high-, medium- and low- dose XZCBF treatment groups, respectively, showing a dose-dependent pattern and a statistically significant difference from the concentrations in the model group ($P < 0.05$). No differences were identified in either the high- or medium- dose XZCBF treatment group or the benzbromarone treatment group regarding the level of uric acid ($P < 0.05$); however, a significant difference was found between the low- dose XZCBF treatment group and the benzbromarone treatment group ($P < 0.05$).

3.4. qRT-PCR analysis of URAT1 and miR-34a in kidney tissue

The relative sample template quantities ($2^{-\Delta\Delta Ct}$) of URAT1 were calculated and compared between the groups. The original standard error of URAT1 $2^{-\Delta\Delta Ct}$ was too large, thus, the values were converted to square roots. Based on ANOVA, the URAT1 expression level (2.89 ± 1.13) in the blank control group was significantly lower than that in the other groups ($P < 0.05$), with the exception of the benzbromarone group. The URAT1 expression levels in the high-, medium- and low- dose XZCBF treatment groups and the benzbromarone treatment group were 5.17 ± 2.17, 7.91 ± 2.40, 8.67 ± 2.71, and 4.58 ± 0.56, respectively, all of which were lower than that in the model group (16.82 ± 3.05, $P < 0.05$). The expression of URAT1 showed a dose-dependent pattern in the three XZCBF treatment groups, and no difference was noted between either the high- dose

Table 3
The expression quantities of URAT1 and miR-34a in mouse kidney tissues.

Groups	*N*	URAT1 $2^{-\triangle\triangle Ct}$ (SQRT)	miR-34a $2^{-\triangle\triangle Ct}$
XZCBF high dose	10	$5.17 \pm 2.17^{*\triangle}$	$6.46 \pm 2.19^{*\triangle}$
XZCBF medium dose	10	$7.91 \pm 2.40^{*\triangle}$	$6.40 \pm 1.28^{*\triangle}$
XZCBF low dose	10	$8.67 \pm 2.71^{*}$	$5.60 \pm 0.93^{*\triangle}$
Benzbromarone	10	$4.58 \pm 0.56^{*}$	$6.66 \pm 1.45^{*}$
model	10	16.82 ± 3.05	1.61 ± 0.46
Blank control	10	$2.89 \pm 1.13^{*}$	$10.32 \pm 4.73^{*}$

$^{\triangle}$Ct=target gene Ct-internal control Ct; $^{\triangle\triangle}$Ct=target gene in the tested sample $^{\triangle}$Ct-target gene in the control sample $^{\triangle}$Ct (choose the sample with the highest $^{\triangle}$Ct if no control was included); when the amplification efficiency of PCR reached 100%; the relative sample template quantity=$2^{-\triangle\triangle Ct}$.

* $P < 0.05$ compared with Model; $^{\triangle}P > 0.05$ compared with benzbromarone.

XZCBF treatment group or the benzbromarone treatment group and the blank control group regarding the mRNA expression level of URAT1 (Table 3).

The relative sample template quantities ($2^{-\triangle\triangle Ct}$) of miR-34a were calculated and compared between the groups. According to the results of ANOVA, the level of miR-34a expression in the blank control group (10.32 ± 4.73) was significantly higher than that in the other 5 groups ($P < 0.05$). The levels of miR-34a expression in the high-, medium- and low- dose XZCBF treatment groups and the benzbromarone treatment group were 6.46 ± 2.19, 6.40 ± 1.28, 5.60 ± 0.93, and 6.66 ± 1.45, respectively, all of which were higher than that in the model group (1.61 ± 0.46; $P < 0.05$). The expression of miR-34a exhibited a dose-dependent pattern in the three XZCBF treatment groups, and no difference in the expression level

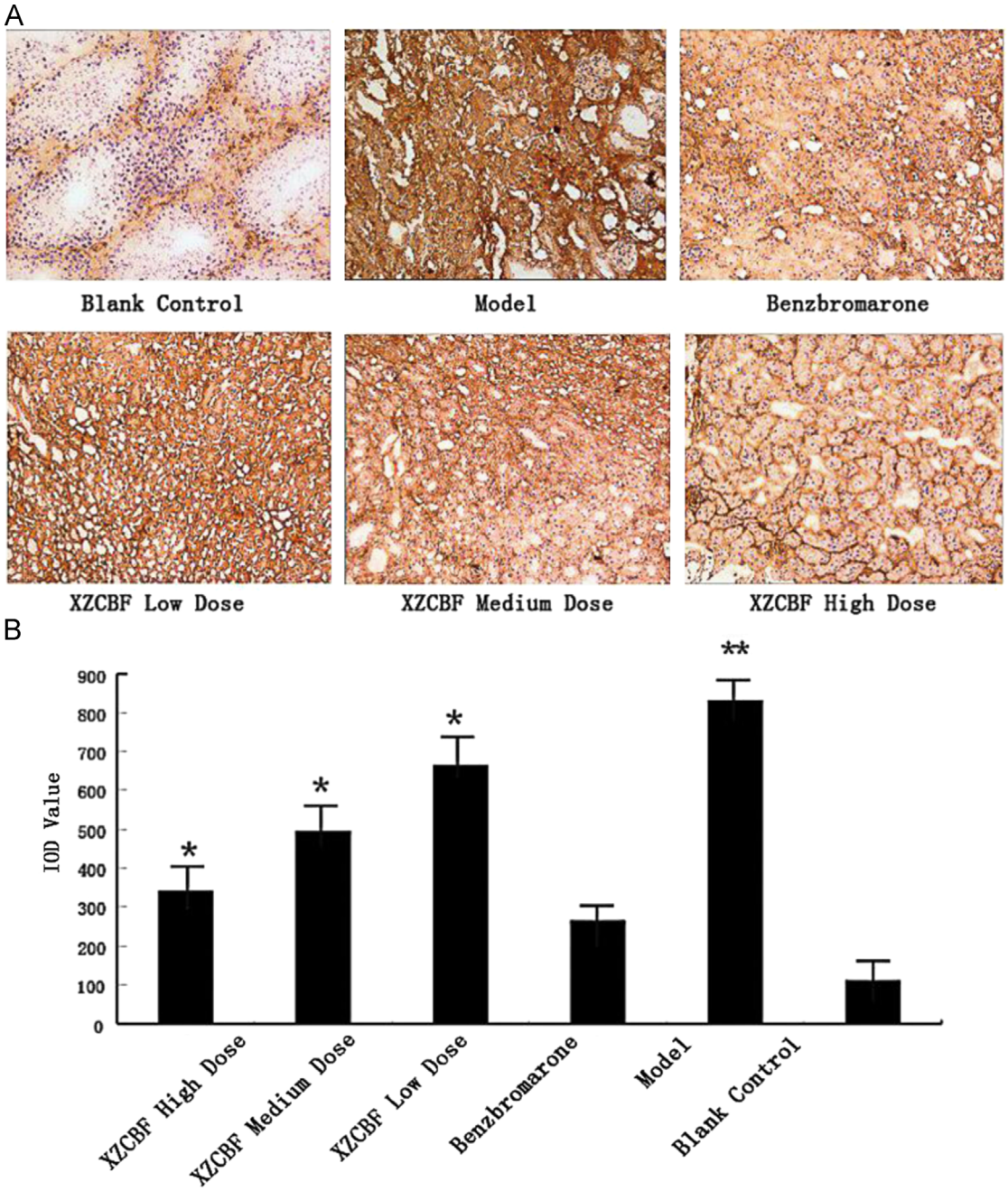

Fig. 2. The mRNA Expression of URAT1 in renal tissues by immunohistochemistry and in situ hybridization. (A) Immunohistochemistry and in situ hybridization results. (B) Analysis of digital images of URAT1 results by IOD. *$P < 0.05$, compared with model. **$P < 0.05$, compared with blank control.

of miR-34a was noted between the three XZCBF treatment groups and the benzbromarone treatment group (Table 3).

3.5. Correlation analysis

We performed Pearson's correlation analysis between the uric acid levels and the expression levels of URAT1 in the experimental mice ($r=0.766$, $P=0.000$, $P<0.05$). The uric acid level was positively correlated with the expression levels of URAT1 mRNA. Additionally, we performed Pearson's correlation analysis between the expression levels of URAT1 and miR-34a ($r=-0.582$, $P=0.000$, $P<0.05$), and we found that the expression level of URAT1 was negatively correlated with that of miR-34a.

3.6. Immunohistochemical staining, in situ hybridization and correlation analysis

The analysis of digital images of URAT1 immunohistochemistry results, by IOD, revealed that the intergroup difference in URAT1 expression levels was significant ($P<0.05$). The levels of URAT1 expression in the high-, medium-, and low- dose XZCBF treatment groups were lower than that in the model group (Fig. 2A and B), while

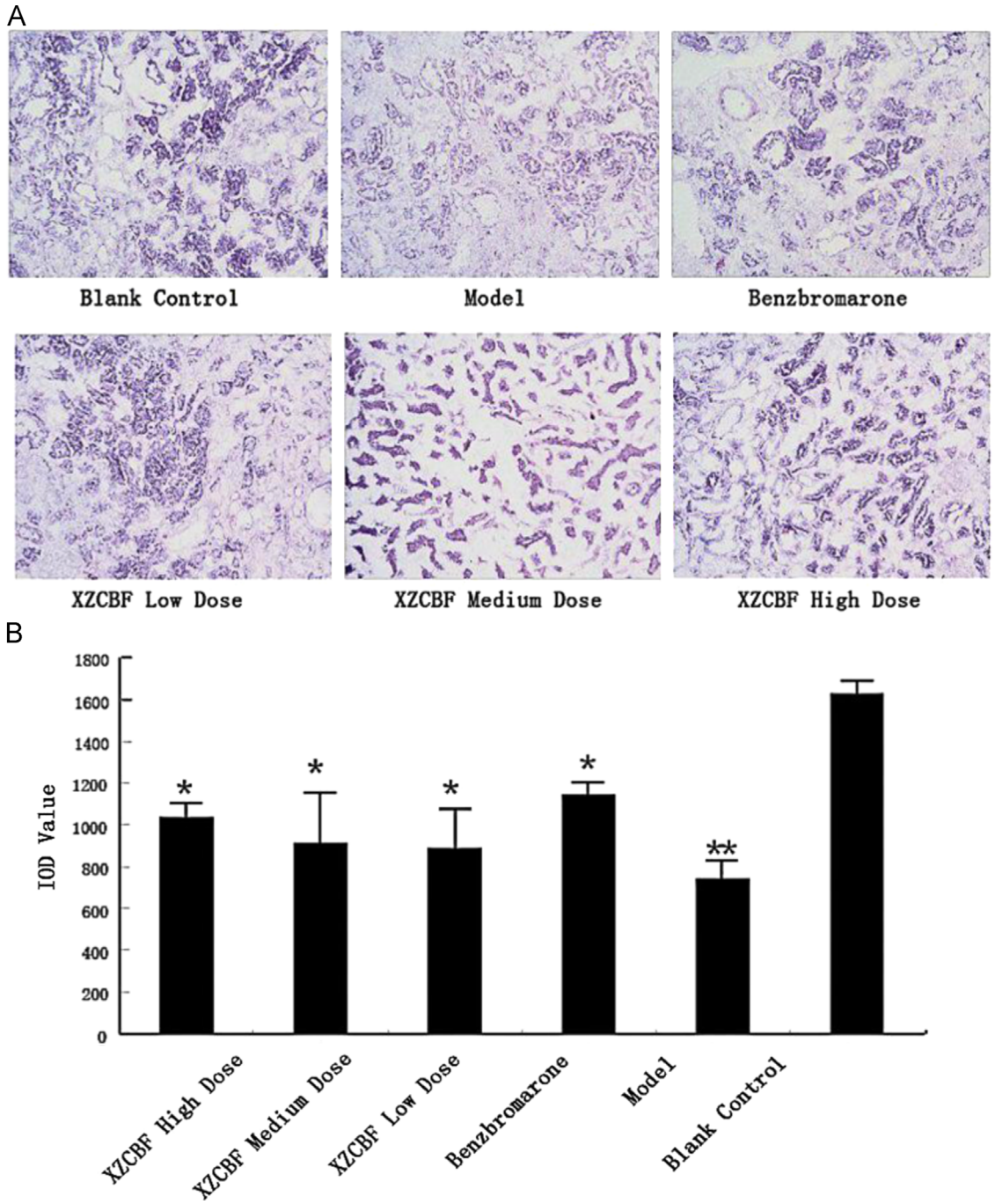

Fig. 3. The Has-mir-34a expression in renal tissues by immunohistochemistry and in situ hybridization. (A) Immunohistochemistry and in situ hybridization results. (B) Analysis of digital images of Has-mir-34a results by IOD. $^{*}P<0.05$, compared with model. $^{**}P<0.05$, compared with blank control.

the levels of miR-34a expression in the high-, medium-, and low- dose XZCBF treatment groups were higher than that in the model group, indicating that XZCBF may induce the expression of miR-34a in kidney tissue (Fig. 3A and B). This result was consistent with the gene expression results reported above, with a similar correlation analysis result ($r=0.656$, $P=0.000$).

4. Discussion

Our experiments showed that miR-34a could inhibit the expression of URAT1 and that the target site of miR-34a was located at position 331–338 of SLC22A12-3′UTR. Moreover, the results also demonstrated that the high, medium, and low doses of XZCBF all lowered the uric acid levels in the hyperuricemic mice model. URAT1 and miR-34a were universally expressed in kidney tissue in each group; however, the mRNA expression of URAT1 tended to decrease with an increase in the therapeutic dose of XZCBF, while the expression of miR-34a tended to increase. A dose-dependent relationship between the uric acid level, URAT1, and miR-34a was clearly present in all three XZCBF treatment groups. This relationship was further supported by the results of immunohistochemistry and in situ hybridization. Pearson's correlation analysis showed that the mRNA expression levels of URAT1 were positively correlated with the uric acid level, but negatively correlated with miR-34a expression.

Hyperuricemic animal models are important tools for studying uric acid metabolism and associated diseases. Because uric acid can be further degraded into allantoin by uricase in rodents, but not in humans, it is not easy to create hyperuricemic models in these animals. Because hyperuricemia is mainly caused by a high intake of purine-rich food, to reduce the interspecies difference between humans and mice, we created a hyperuricemic model by administering 97% allantoxanic acid potassium salt and adenine by gavage, employing the procedures described in previous studies (Chen and Xu, 2004; Tong et al., 2009) with some modifications. This model closely mimics the manner in which hyperuricemia emerges in humans, and its success was supported by the clearly elevated uric acid levels observed in our study.

According to the theory of TCM, dampness turbidity (Shizhuo) and phlegm-static blood (Tanyu) are thought to be the major factors in the pathogenesis of hyperuricemia. Innate insufficiencies, cause deficiencies in the “Kidney” and “Spleen”, reduced transport, the generation of dampness turbidity, and the blocking of “Qi” and “Blood”. The blockage of “Blood” leads to a static combination of phlegm and static blood, which is a tedious process that involves the “Kidney”. XZCBF facilitates the excretion of dampness turbidity and the removal of phlegm-static blood to cure hyperuricemia and gout. Our study results showed that oral administration of XZCBF lowered uric acid levels in a hyperuricemic mice model and that high-dose treatment was comparable to benzbromarone treatment; however, medium- and low- dose XZCBF treatment was not as effective, indicating that sufficient doses and therapeutic durations during clinical application could ensure satisfactory clinical efficacy. Our previous studies also demonstrated that XZCBF was similar to benzbromarone with respect to its ability to inhibit the reabsorption of uric acid mediated by URAT1.

5. Conclusions

In summary, we conclude that XZCBF can significantly lower uric acid levels in a hyperuricemic animal model, which may be mediated by its capacity to upregulate miR-34a to suppress URAT1, resulting in improved excretion of uric acid. Thus, XZCBF may play a role in the treatment of hyperuricemia.

Acknowledgments

This project was supported by the National Natural Science Foundation of China (No.81072915), Guangdong Major Science and Technology Projects (No.2012A080201012), and the Guangdong Provincial Natural Science Foundation (No.S2012010009032).

References

Chen, G.L., Xu, S.Y., 2004. Research progress for animal hyperuricemia model. Chinese Pharmacological Bulletin 20, 369.
Cheong, H.I., Kang, J.H., Lee, J.H., Ha, I.S., Kim, S., Komoda, F., et al., 2008. Mutational analysis of idiopathic renal hypouricemia in Korea. Pediatric Nephrology 20, 886–890.
Chinese Pharmacopoeia Commission, 2010. Pharmacopoeia of the People's Republic of China. China Medical Science Press, China, 17, 31, 49, 67, 271.
Crittenden, D.B., Lehmann, R.A., Schneck, L., et al., 2012. Colchicine use is associated with decreased prevalence of myocardial infarction in patients with gout. The Journal of Rheumatology 39, 1458–1464.
Fei, H.R., Gao, Y.S., Mao, Y.H., et al., 2005. Anti-inflammatory and analgesic effects of aqueous extract from *dioscorea collettii* Var. Chinese Journal of Clinical Rehabilitation 39, 110–111.
Fei, H.R., Mao, Y.H., Zhu, W., et al., 2007. Elimination Effects of *Dioscorea collettii* Hook Var on Uric Acid. Herald of Medicine 11, 1270–1272.
Gao, C.K., Gao, J., RL, M.A., et al., 2003. Research on analgesic and anti-inflammatory and invigorate circulation effects of total saponins of *Achyranthes*. Anhui Medical and Pharmaceutical Journal 7, 248–249.
Hong, Q., Wu, D., Chen, X.M., Hou, K., Feng, Z., Fu, B., et al., 2005. Location and expression of human uric acid transporter in HKC. Chinese Journal of Nephrology 21, 527–533.
Jing, H.E., Niu, C.Q., Hu, J.M., et al., 2007. Vasodilatation effects of the water decoction of *Vaccaria Segetalis* (Neck) Garcke on rabbit aorta in vitro. Journal of Sichuan of Traditional Chinese Medicine 8, 13–15.
Lewis, B.P., Burge, C.B., Bartel, D.P., 2005. Conserved seed pairing, often flanked by adenosines, indicates that thousands of human genes are microRNA targets. Cell 120, 15–20.
Liu, Z.G., Deng, W.J., Zheng, P.C., Sun, W.F., Wu, X.R., 2011a. Study on extracting and alcohol precipitating craft of compound Tufuling granules. Chinese Archives of Traditional Chinese Medicine 29, 1594–1595.
Liu, Z.G., Deng, W.J., Sun, W.F., Wu, X.R., 2011b. Studies on the quality and quantity analysis methods of compound Tufuling granules. Chinese Journal of Pharmaceutical Analalysis 31, 119–123.
Li, Z.K., Li, D.D., 1997. The immunomodulatory effect of *Achyranthes bidentata* polysaccharides. Acta Pharmaceutica Sinica B 12, 881–887.
Nadeau, I., Kamen, A., 2003. Production of adenovirus vector for gene therapy. Biotechnology Advances 20, 475–489.
Roddy, E., Zhang, W., Doherty, M., 2007. The changing epidemiology of gout. Nature Clinical Practice Rheumatology 3, 443–449.
Shi, Y., Yang, Y.L., Li, W.Y., et al., 2012. Extraction the colchicine of *Iphigenia indica* in aqueous two-phase System. Natural Product Research and Development 24, 1412–1416.
Sun, W.F., Zhang, X.X., Xu, W., 2009. Therapeutic effect of two compositions of Xiezhuo Chubi decoction on primary gout hyperuricemia. Military Medical Journal of South China 23, 35.
Sun, W.F., Zhang, X.X., Sun, F.Y., et al., 2011. MicroRNA expression patterns in the kidney of mice treated with XZCBF. Chinese Journal of Integrative Medicine 17, 35–42.
Tong, G.H., Yi, Zhang, Ma, L., 2009. Research progress for rodent hyperuricemia model. Journal of Toxicology 23, 159–162.
Wang, F., 2004. Research progress for urate transporters in renal. Foreign Medical Sciences (Section of Endocrinology) 24, 388–390.
Wu, E.Q., P.A. Patel, Yu AP, et al., 2008. Disease-related and all-cause health care costs of elderly patients with gout. Journal of Managed Care Pharmacy 14, 164–175.
Wu, L.G., Fan, J.H., Belasco, J.G., 2006. MicroRNAs direct rapid deadenylation of mRNA. Proceedings of the National Academy of the United States of America 103, 4034–4039.
Zhang, B.J., Liu, Y.O., Liu, L., et al., 2004. Study on anti-inflammatory, analgesic, diuretic effect of *smilax glabra* and astilbin. Pharmacology and Clinics of Chinese Materia Medica 20, 11–12.